
Classic GNNs are Strong Baselines: Reassessing GNNs for Node Classification

Yuankai Luo

Beihang University
The Hong Kong Polytechnic University
luoyk@buaa.edu.cn

Lei Shi

Beihang University
leishi@buaa.edu.cn

Xiao-Ming Wu

The Hong Kong Polytechnic University
xiao-ming.wu@polyu.edu.hk

Abstract

Graph Transformers (GTs) have recently emerged as popular alternatives to traditional message-passing Graph Neural Networks (GNNs), due to their theoretically superior expressiveness and impressive performance reported on standard node classification benchmarks, often significantly outperforming GNNs. In this paper, we conduct a thorough empirical analysis to reevaluate the performance of three classic GNN models (GCN, GAT, and GraphSAGE) against GTs. Our findings suggest that the previously reported superiority of GTs may have been overstated due to suboptimal hyperparameter configurations in GNNs. Remarkably, with slight hyperparameter tuning, these classic GNN models achieve state-of-the-art performance, matching or even exceeding that of recent GTs across 17 out of the 18 diverse datasets examined. Additionally, we conduct detailed ablation studies to investigate the influence of various GNN configurations—such as normalization, dropout, residual connections, network depth, and jumping knowledge mode—on node classification performance. Our study aims to promote a higher standard of empirical rigor in the field of graph machine learning, encouraging more accurate comparisons and evaluations of model capabilities. Our implementation is available at <https://github.com/LUOyk1999/tunedGNN>.

1 Introduction

Node classification is a fundamental task in graph machine learning, with high-impact applications across many fields such as social network analysis, bioinformatics, and recommendation systems. Graph Neural Networks (GNNs) [20, 28, 65, 72, 49, 33, 8, 76, 18, 9, 51, 4, 73, 56, 10, 52, 53, 66, 77, 37] have emerged as a powerful class of models for tackling the node classification task. GNNs operate by iteratively aggregating information from a node’s neighbors, a process known as message passing [19], leveraging both the graph structure and node features to learn useful node representations for classification. While GNNs have achieved notable success, studies have identified several limitations, including over-smoothing [35], over-squashing [1], lack of sensitivity to heterophily [81], and challenges in capturing long-range dependencies [11].

Recently, Graph Transformers (GTs) [50, 48, 23] have gained prominence as popular alternatives to GNNs. Unlike GNNs, which primarily aggregate local neighborhood information, the Transformer architecture [64] can capture interactions between any pair of nodes via a self-attention layer. GTs have achieved significant success in graph-level tasks, e.g., graph classification involving small-scale graphs like molecular graphs [13, 74, 30, 42, 55, 6]. This success has inspired efforts

[12, 17, 71, 70, 69, 79, 82, 15, 60, 7, 29, 40, 38] to utilize GTs to tackle node classification tasks, especially on large-scale graphs, addressing the aforementioned limitations of GNNs. While recent advancements in state-of-the-art GTs [12, 71] have shown promising results, it’s observed that many of these models, whether explicitly or implicitly, still rely on GNNs for learning local node representations, integrating them alongside the global attention mechanisms for a more comprehensive representation.

This prompts us to reconsider: *Could the potential of message-passing GNNs for node classification have been previously underestimated?* While prior research has addressed this issue to some extent [24, 14, 68, 44, 54], these studies have limitations in terms of scope and comprehensiveness, including a restricted number and diversity of datasets, as well as an incomplete examination of hyperparameters. In this study, we comprehensively reassess the performance of GNNs for node classification, utilizing three classic GNN models—GCN [28], GAT [64], and GraphSAGE [20]—across 18 real-world benchmark datasets that include homophilous, heterophilous, and large-scale graphs. We examine the influence of key hyperparameters on GNN training, including normalization [2, 26], dropout [63], residual connections [21], network depth, and the utilization of the jumping knowledge mode [73]. We summarize the key findings in our empirical study as follows:

- With proper hyperparameter tuning, classic GNNs can achieve highly competitive performance in node classification across homophilous and heterophilous graphs with up to millions of nodes. Notably, classic GNNs outperform state-of-the-art GTs, achieving the top rank on 17 out of 18 datasets. This indicates that the previously claimed superiority of GTs over GNNs may have been overstated, possibly due to suboptimal hyperparameter configurations in GNN evaluations.
- Our ablation studies have yielded valuable insights into GNN hyperparameters for node classification. We demonstrate that (1) normalization is essential for large-scale graphs; (2) dropout consistently proves beneficial; (3) residual connections can significantly enhance performance, especially on heterophilous graphs; (4) GNNs on heterophilous graphs tend to perform better with deeper layers; and (5) jumping knowledge connections have minimal impact on large-scale graphs.

2 Classic GNNs for Node Classification

Define a graph as $\mathcal{G} = (\mathcal{V}, \mathcal{E}, \mathbf{X}, \mathbf{Y})$, where \mathcal{V} denotes the set of nodes, $\mathcal{E} \subseteq \mathcal{V} \times \mathcal{V}$ represents the set of edges, $\mathbf{X} \in \mathbb{R}^{|\mathcal{V}| \times d}$ is the node feature matrix, with $|\mathcal{V}|$ representing the number of nodes and d the dimension of the node features, and $\mathbf{Y} \in \mathbb{R}^{|\mathcal{V}| \times C}$ is the one-hot encoded label matrix, with C being the number of classes. Let $\mathbf{A} \in \mathbb{R}^{|\mathcal{V}| \times |\mathcal{V}|}$ denote the adjacency matrix of \mathcal{G} .

Message Passing Graph Neural Networks (GNNs) [19] compute node representations \mathbf{h}_v^l at each layer l as:

$$\mathbf{h}_v^l = \text{UPDATE}^l \left(\mathbf{h}_v^{l-1}, \text{AGG}^l \left(\left\{ \mathbf{h}_u^{l-1} \mid u \in \mathcal{N}(v) \right\} \right) \right), \quad (1)$$

where $\mathcal{N}(v)$ represents the neighboring nodes adjacent to v , AGG^l serves as the message aggregation function, and UPDATE^l is the update function. Initially, each node v begins with a feature vector $\mathbf{h}_v^0 = \mathbf{x}_v \in \mathbb{R}^d$. The function AGG^l aggregates information from the neighbors of v to update its representation. The output of the last layer L , i.e., $\text{GNN}(v, \mathbf{A}, \mathbf{X}) = \mathbf{h}_v^L$, is the representation of v produced by the GNN. In this work, we focus on three classic GNNs: GCN [28], GraphSAGE [20], and GAT [64], which differ in their approach to learning the node representation \mathbf{h}_v^l .

Graph Convolutional Networks (GCN) [28], the standard GCN model, is formulated as:

$$\mathbf{h}_v^l = \sigma \left(\sum_{u \in \mathcal{N}(v) \cup \{v\}} \frac{1}{\sqrt{\hat{d}_u \hat{d}_v}} \mathbf{h}_u^{l-1} \mathbf{W}^l \right), \quad (2)$$

where $\hat{d}_v = 1 + \sum_{u \in \mathcal{N}(v)} 1$, $\sum_{u \in \mathcal{N}(v)} 1$ denotes the degree of node v , \mathbf{W}^l is the trainable weight matrix in layer l , and σ is the activation function, e.g., $\text{ReLU}(\cdot) = \max(0, \cdot)$.

GraphSAGE [20] learns node representations through a different approach:

$$\mathbf{h}_v^l = \sigma(\mathbf{h}_v^{l-1} \mathbf{W}_1^l + (\text{mean}_{u \in \mathcal{N}(v)} \mathbf{h}_u^{l-1}) \mathbf{W}_2^l), \quad (3)$$

where \mathbf{W}_1^l and \mathbf{W}_2^l are trainable weight matrices, and $\text{mean}_{u \in \mathcal{N}(v)} \mathbf{h}_u^{l-1}$ computes the average embedding of the neighboring nodes of v .

Graph Attention Networks (GAT) [64] employ masked self-attention to assign weights to different neighboring nodes. For an edge $(v, u) \in \mathcal{E}$, the propagation rule of GAT is defined as:

$$\alpha_{vu}^l = \frac{\exp\left(\text{LeakyReLU}\left(\mathbf{a}_l^\top \left[\mathbf{W}^l \mathbf{h}_v^{l-1} \parallel \mathbf{W}^l \mathbf{h}_u^{l-1}\right]\right)\right)}{\sum_{r \in \mathcal{N}(v)} \exp\left(\text{LeakyReLU}\left(\mathbf{a}_l^\top \left[\mathbf{W}^l \mathbf{h}_v^{l-1} \parallel \mathbf{W}^l \mathbf{h}_r^{l-1}\right]\right)\right)},$$

$$\mathbf{h}_v^l = \sigma\left(\sum_{u \in \mathcal{N}(v)} \alpha_{vu}^l \mathbf{h}_u^{l-1} \mathbf{W}^l\right), \quad (4)$$

where \mathbf{a}_l is a trainable weight vector, \mathbf{W}^l is a trainable weight matrix, and \parallel represents the concatenation operation.

Node Classification aims to predict the labels of the unlabeled nodes. Typically, for any node v , the node representation generated by the last GNN layer is passed through a prediction head $g(\cdot)$, to obtain the predicted label $\hat{\mathbf{y}}_v = g(\text{GNN}(v, \mathbf{A}, \mathbf{X}))$. The training objective is to minimize the total loss $L(\theta) = \sum_{v \in \mathcal{V}_{\text{train}}} \ell(\hat{\mathbf{y}}_v, \mathbf{y}_v)$ w.r.t. all nodes in the training set $\mathcal{V}_{\text{train}}$, where \mathbf{y}_v indicates the ground-truth label of v and θ indicates the trainable GNN parameters.

Homophilous and Heterophilous Graphs. Node classification can be performed on both homophilous and heterophilous graphs. Homophilous graphs are characterized by edges that tend to connect nodes of the same class, while in heterophilous graphs, connected nodes may belong to different classes [54]. GNN models implicitly assume homophily in graphs [45], and it is commonly believed that due to this homophily assumption, GNNs cannot generalize well to heterophilous graphs [81, 9]. However, recent works [43, 39, 54, 41] have empirically shown that standard GCNs also work well on heterophilous graphs. In this study, we provide a comprehensive evaluation of classic GNNs for node classification on both homophilous and heterophilous graphs.

3 Key Hyperparameters for Training GNNs

In this section, we present an overview of the key hyperparameters for training GNNs, including normalization, dropout, residual connections, network depth, and ‘‘jumping knowledge’’ mode. The first four hyperparameters are widely utilized across different types of neural networks to improve model performance, while the last one is specific to GNNs.

Normalization. Specifically, Layer Normalization (LN) [2] or Batch Normalization (BN) [26] can be used in every layer before the activation function $\sigma(\cdot)$. Taking GCN as an example:

$$\mathbf{h}_v^l = \sigma\left(\text{Norm}\left(\sum_{u \in \mathcal{N}(v) \cup \{v\}} \frac{1}{\sqrt{\hat{d}_u \hat{d}_v}} \mathbf{h}_u^{l-1} \mathbf{W}^l\right)\right). \quad (5)$$

The normalization techniques are essential for stabilizing the training process by reducing the *covariate shift*, which occurs when the distribution of each layer’s node embeddings changes during training. Normalizing the node embeddings helps to maintain a more consistent distribution, allowing the use of higher learning rates and leading to faster convergence [5].

Dropout [63], a technique widely used in convolutional neural networks (CNNs) to address overfitting by reducing co-adaptation among hidden neurons [22, 75], has also been found to be effective in addressing similar issues in GNNs [64, 61], where the co-adaptation effects propagate and accumulate through message passing among different nodes. Typically, dropout is applied to the feature embeddings after the activation function:

$$\mathbf{h}_v^l = \text{Dropout}\left(\sigma\left(\text{Norm}\left(\sum_{u \in \mathcal{N}(v) \cup \{v\}} \frac{1}{\sqrt{\hat{d}_u \hat{d}_v}} \mathbf{h}_u^{l-1} \mathbf{W}^l\right)\right)\right). \quad (6)$$

Residual Connections [21] significantly enhance CNN performance by connecting layer inputs directly to outputs, thereby alleviating the vanishing gradient issue. They were first adopted by the seminal GCN paper [28] and subsequently incorporated into DeepGCNs [33] to boost performance. Formally, linear residual connections can be integrated into GNNs as follows:

$$\mathbf{h}_v^l = \text{Dropout}\left(\sigma\left(\text{Norm}\left(\mathbf{h}_v^{l-1} \mathbf{W}_r^l + \sum_{u \in \mathcal{N}(v) \cup \{v\}} \frac{1}{\sqrt{\hat{d}_u \hat{d}_v}} \mathbf{h}_u^{l-1} \mathbf{W}^l\right)\right)\right), \quad (7)$$

Table 1: Overview of the datasets used for node classification.

Dataset	Type	# nodes	# edges	# Features	Classes	Metric
Cora	Homophily	2,708	5,278	2,708	7	Accuracy
CiteSeer	Homophily	3,327	4,522	3,703	6	Accuracy
PubMed	Homophily	19,717	44,324	500	3	Accuracy
Computer	Homophily	13,752	245,861	767	10	Accuracy
Photo	Homophily	7,650	119,081	745	8	Accuracy
CS	Homophily	18,333	81,894	6,805	15	Accuracy
Physics	Homophily	34,493	247,962	8,415	5	Accuracy
WikiCS	Homophily	11,701	216,123	300	10	Accuracy
Squirrel	Heterophily	5,201	216,933	2,089	5	Accuracy
Chameleon	Heterophily	2,277	36,101	2,325	5	Accuracy
Roman-Empire	Heterophily	22,662	32,927	300	18	Accuracy
Amazon-Ratings	Heterophily	24,492	93,050	300	5	Accuracy
Minesweeper	Heterophily	10,000	39,402	7	2	ROC-AUC
Questions	Heterophily	48,921	153,540	301	2	ROC-AUC
ogbn-proteins	Homophily (Large graphs)	132,534	39,561,252	8	2	ROC-AUC
ogbn-arxiv	Homophily (Large graphs)	169,343	1,166,243	128	40	Accuracy
ogbn-products	Homophily (Large graphs)	2,449,029	61,859,140	100	47	Accuracy
pokec	Heterophily (Large graphs)	1,632,803	30,622,564	65	2	Accuracy

where \mathbf{W}_r^l is a trainable weight matrix. This configuration mitigates gradient instabilities and enhances GNN expressiveness [72], addressing the over-smoothing [35] and oversquashing [1] issues since the linear component ($\mathbf{h}_u^{l-1} \mathbf{W}_r^l$) helps to preserve distinguishable node representations [68].

Network Depth. Deeper network architectures, such as deep CNNs [21, 25], are capable of extracting more complex, high-level features from data, potentially leading to better performance on various prediction tasks. However, GNNs face unique challenges with depth, such as over-smoothing [35], where node representations become indistinguishable with increased network depth. Consequently, in practice, most GNNs adopt a shallow architecture, typically consisting of 2 to 5 layers. While previous research, such as DeepGCN [33] and DeeperGCN [34], advocates the use of deep GNNs with up to 56 and 112 layers, our findings indicate that comparable performance can be achieved with significantly shallower GNN architectures, typically ranging from 2 to 10 layers.

Jumping Knowledge (JK) Mode [73] aggregates representations from different GNN layers, effectively capturing information from varying neighborhood ranges within the graph. For any node v , the summation version of JK mode produces the representation of v by:

$$\text{GNN}_{\text{JK}}(v, \mathbf{A}, \mathbf{X}) = \mathbf{h}_v^1 + \mathbf{h}_v^2 + \dots + \mathbf{h}_v^L, \quad (8)$$

where L is the number of GNN layers.

4 Experimental Setup for Node Classification

Datasets. Table 1 presents a summary of the statistics and characteristics of the datasets.

- **Homophilous Graphs.** **Cora**, **CiteSeer**, and **PubMed** are three widely used citation networks [58]. We follow the semi-supervised setting of [28] for data splits and metrics. Additionally, **Computer** and **Photo** [59] are co-purchase networks where nodes represent goods and edges indicate that the connected goods are frequently bought together. **CS** and **Physics** [59] are co-authorship networks where nodes denote authors and edges represent that the authors have co-authored at least one paper. We adhere to the widely accepted practice of training/validation/test splits of 60%/20%/20% and metric of accuracy [7, 60, 12]. Furthermore, we utilize the **WikiCS** dataset and use the official splits and metrics provided in [47].
- **Heterophilous Graphs.** **Squirrel** and **Chameleon** [57] are two well-known page-page networks that focus on specific topics in Wikipedia. According to the heterophilous graphs benchmarking paper [54], the original split of these datasets introduces overlapping nodes between training and testing, leading to the proposal of a new data split that filters out the overlapping nodes. We use its provided split and its metrics for evaluation. Additionally, we utilize four other heterophilous datasets proposed by the same source [54]: **Roman-Empire**, where nodes correspond to words in the Roman Empire Wikipedia article and edges connect sequential or syntactically

Table 2: Node classification results over homophilous graphs (%). * indicates our implementation, while other results are taken from [12, 71]. The top 1st, 2nd and 3rd results are highlighted.

	Cora	CiteSeer	PubMed	Computer	Photo	CS	Physics	WikiCS
# nodes	2,708	3,327	19,717	13,752	7,650	18,333	34,493	11,701
# edges	5,278	4,732	44,324	245,861	119,081	81,894	247,962	216,123
Metric	Accuracy↑	Accuracy↑	Accuracy↑	Accuracy↑	Accuracy↑	Accuracy↑	Accuracy↑	Accuracy↑
GraphGPS	82.84 ± 1.03	72.73 ± 1.23	79.94 ± 0.26	91.19 ± 0.54	95.06 ± 0.13	93.93 ± 0.12	97.12 ± 0.19	78.66 ± 0.49
NAGphormer	82.12 ± 1.18	71.47 ± 1.30	79.73 ± 0.28	91.22 ± 0.14	95.49 ± 0.11	95.75 ± 0.09	97.34 ± 0.03	77.16 ± 0.72
Expformer	82.77 ± 1.38	71.63 ± 1.19	79.46 ± 0.35	91.47 ± 0.17	95.35 ± 0.22	94.93 ± 0.01	96.89 ± 0.09	78.54 ± 0.49
GOAT	83.18 ± 1.27	71.99 ± 1.26	79.13 ± 0.38	90.96 ± 0.90	92.96 ± 1.48	94.21 ± 0.38	96.24 ± 0.24	77.00 ± 0.77
NodeFormer	82.20 ± 0.90	72.50 ± 1.10	79.90 ± 1.00	86.98 ± 0.62	93.46 ± 0.35	95.64 ± 0.22	96.45 ± 0.28	74.73 ± 0.94
SGFormer	84.50 ± 0.80	72.60 ± 0.20	80.30 ± 0.60	91.99 ± 0.76	95.10 ± 0.47	94.78 ± 0.20	96.60 ± 0.18	73.46 ± 0.56
Polynormer	83.25 ± 0.93	72.31 ± 0.78	79.24 ± 0.43	93.68 ± 0.21	96.46 ± 0.26	95.53 ± 0.16	97.27 ± 0.08	80.10 ± 0.67
GCN	81.60 ± 0.40	71.60 ± 0.40	78.80 ± 0.60	89.65 ± 0.52	92.70 ± 0.20	92.92 ± 0.12	96.18 ± 0.07	77.47 ± 0.85
GCN*	85.08 ± 0.52	3.48 †	72.98 ± 0.84	1.38 †	81.32 ± 0.72	2.52 †	93.80 ± 0.29	4.15 †
GraphSAGE	82.68 ± 0.47	71.93 ± 0.85	79.41 ± 0.53	91.20 ± 0.29	94.59 ± 0.14	93.91 ± 0.13	96.49 ± 0.06	74.77 ± 0.95
GraphSAGE*	84.18 ± 0.81	1.50 †	71.93 ± 0.85	0.00 †	79.41 ± 0.53	0.00 †	93.59 ± 0.22	2.39 †
GAT	83.00 ± 0.70	72.10 ± 1.10	79.00 ± 0.40	90.78 ± 0.13	93.87 ± 0.11	93.61 ± 0.14	96.17 ± 0.08	76.91 ± 0.82
GAT*	84.64 ± 1.27	1.64 †	72.10 ± 1.10	0.00 †	79.70 ± 0.70	0.70 †	93.93 ± 0.16	3.15 †
					96.67 ± 0.13	2.80 †	96.08 ± 0.10	2.47 †
							97.30 ± 0.06	1.13 †
								80.75 ± 0.74
								3.84 †

linked words; **Amazon-Ratings**, where nodes represent products and edges connect frequently co-purchased items; **Minesweeper**, a synthetic dataset where nodes are cells in a 100×100 grid and edges connect neighboring cells; and **Questions**, where nodes represent users from the Yandex Q question-answering website and edges connect users who interacted through answers. All splits and evaluation metrics are consistent with those proposed in the source.

- **Large-scale Graphs.** We consider a collection of large graphs released recently by the Open Graph Benchmark (OGB) [24]: **ogbn-arxiv**, **ogbn-proteins**, and **ogbn-products**, with node numbers ranging from 0.16M to 2.4M. We maintain all the OGB standard evaluation settings. Additionally, we analyze performance on the social network **pokec** [32], which has 1.6M nodes, following the evaluation settings of [12].

Baselines. Our main focus lies on classic GNNs: **GCN** [28], **GraphSAGE** [20], **GAT** [64], the state-of-the-art scalable GTs: **SGFormer** [71], **Polynormer** [12], **GOAT** [29], **NodeFormer** [70], **NAGphormer** [7], and powerful GTs: **GraphGPS** [55] and **Expformer** [60]. Furthermore, various other GTs like [17, 15, 38, 78, 31, 3, 6, 74, 13] exist in related surveys [23, 50], empirically shown to be inferior to the GTs we compared against for node classification tasks. For heterophilous graphs, We also consider five models designed for node classification under heterophily following [54]: **H2GCN** [81], **CPGNN** [80], **GPRGNN** [9], **FSGNN** [46], **GloGNN** [36]. Note that we adopt the empirically optimal Polynormer variant (Polynormer-r), which demonstrates superior performance over advanced GNNs such as **LINKX** [37] and **OrderedGNN** [62]. We report the performance results of baselines primarily from [12, 71, 54], with the remaining obtained from their respective original papers or official leaderboards whenever possible, as those results are obtained by well-tuned models.

Hyperparameter Configurations. We conduct minimal hyperparameter tuning on classic GNNs, consistent with the parameter search range of Polynormer [12]. We utilize the Adam optimizer [27] with a learning rate from $\{0.001, 0.005, 0.01\}$ and an epoch limit of 2500. And we tune the hidden dimension from $\{64, 256, 512\}$. As discussed in Section 3, we focus on whether to use normalization (BN or LN), residual connections, jumping knowledge, and dropout rates from $\{0.2, 0.3, 0.5, 0.7\}$, the number of layers from $\{2, 3, 4, 5, 6, 7, 8, 9, 10\}$. Considering the large number of hyperparameters and datasets, we do not perform an exhaustive search. We report mean scores and standard deviations after 5 runs. **GNN*** denotes our implementation of the GNN model.

Detailed experimental setup and hyperparameters are provided in Appendix A.

5 Empirical Findings

5.1 Performance of Classic GNNs in Node Classification

In this subsection, we provide a detailed analysis of the performance of the three classic GNNs compared to state-of-the-art GTs in node classification tasks. Our experimental results across homophilous (Table 2), heterophilous (Table 3), and large-scale graphs (Table 4) reveal that classic GNNs often outperform or match the performance of advanced GTs across 18 datasets. Notably, among the 18 datasets evaluated, classic GNNs achieve the top rank on 17 of them, showcasing their robust competitiveness. We highlight our main observations below.

Table 3: Node classification results on heterophilous graphs (%). * indicates our implementation, while other results are taken from [12, 71, 54]. The top 1st, 2nd and 3rd results are highlighted.

	Squirrel	Chameleon	Amazon-Ratings	Roman-Empire	Minesweeper	Questions
# nodes	2223	890	24,492	22,662	10,000	48,921
# edges	46,998	8,854	93,050	32,927	39,402	153,540
Metric	Accuracy↑	Accuracy↑	Accuracy↑	Accuracy↑	ROC-AUC↑	ROC-AUC↑
H2GCN	35.10 ± 1.15	26.75 ± 3.64	36.47 ± 0.23	60.11 ± 0.52	89.71 ± 0.31	63.59 ± 1.46
CPGNN	30.04 ± 2.03	33.00 ± 3.15	39.79 ± 0.77	63.96 ± 0.62	52.03 ± 5.46	65.96 ± 1.95
GPRGNN	38.95 ± 1.99	39.93 ± 3.30	44.88 ± 0.34	64.85 ± 0.27	86.24 ± 0.61	55.48 ± 0.91
FSGNN	35.92 ± 1.32	40.61 ± 2.97	52.74 ± 0.83	79.92 ± 0.56	90.08 ± 0.70	78.86 ± 0.92
GloGNN	35.11 ± 1.24	25.90 ± 3.58	36.89 ± 0.14	59.63 ± 0.69	51.08 ± 1.23	65.74 ± 1.19
GraphGPS	39.67 ± 2.84	40.79 ± 4.03	53.10 ± 0.42	82.00 ± 0.61	90.63 ± 0.67	71.73 ± 1.47
NodeFormer	38.52 ± 1.57	34.73 ± 4.14	43.86 ± 0.35	64.49 ± 0.73	86.71 ± 0.88	74.27 ± 1.46
SGFormer	41.80 ± 2.27	44.93 ± 3.91	48.01 ± 0.49	79.10 ± 0.32	90.89 ± 0.58	72.15 ± 1.31
Polynormer	40.87 ± 1.96	41.82 ± 3.45	54.81 ± 0.49	92.55 ± 0.37	97.46 ± 0.36	78.92 ± 0.89
GCN	38.67 ± 1.84	41.31 ± 3.05	48.70 ± 0.63	73.69 ± 0.74	89.75 ± 0.52	76.09 ± 1.27
GCN*	44.50 ± 1.92 5.83 ↑	46.11 ± 3.16 4.80 ↑	53.57 ± 0.32 4.87 ↑	91.35 ± 0.37 17.68 ↑	97.77 ± 0.38 8.02 ↑	77.40 ± 1.07 1.31 ↑
GraphSAGE	36.09 ± 1.99	37.77 ± 4.14	53.63 ± 0.39	85.74 ± 0.67	93.51 ± 0.57	76.44 ± 0.62
GraphSAGE*	39.93 ± 1.58 3.84 ↑	43.44 ± 3.19 5.67 ↑	54.72 ± 0.38 1.09 ↑	92.19 ± 0.58 6.45 ↑	96.95 ± 0.41 3.44 ↑	77.96 ± 0.72 1.52 ↑
GAT	35.62 ± 2.06	39.21 ± 3.08	52.70 ± 0.62	88.75 ± 0.41	93.91 ± 0.35	76.79 ± 0.71
GAT*	38.72 ± 1.46 3.10 ↑	43.44 ± 3.00 4.23 ↑	54.99 ± 0.71 2.29 ↑	91.60 ± 0.21 2.85 ↑	97.76 ± 0.37 3.85 ↑	79.04 ± 1.27 2.25 ↑

Table 4: Node classification results on large-scale graphs (%). * indicates our implementation, while other results are taken from [12, 71]. The top 1st, 2nd and 3rd results are highlighted. OOM means out of memory.

	ogbn-proteins	ogbn-arxiv	ogbn-products	pokec
# nodes	132,534	169,343	2,449,029	1,632,803
# edges	39,561,252	1,166,243	61,859,140	30,622,564
Metric	ROC-AUC↑	Accuracy↑	Accuracy↑	Accuracy↑
GraphGPS	76.83 ± 0.26	70.97 ± 0.41	OOM	OOM
GOAT	74.18 ± 0.37	72.41 ± 0.40	82.00 ± 0.43	66.37 ± 0.94
NodeFormer	77.45 ± 1.15	59.90 ± 0.42	72.93 ± 0.13	71.00 ± 1.30
SGFormer	79.53 ± 0.38	72.63 ± 0.13	74.16 ± 0.31	73.76 ± 0.24
NAGphormer	73.61 ± 0.33	70.13 ± 0.55	73.55 ± 0.21	76.59 ± 0.25
Exphormer	74.58 ± 0.26	72.44 ± 0.28	OOM	OOM
Polynormer	78.97 ± 0.47	73.46 ± 0.16	83.82 ± 0.11	86.10 ± 0.05
GCN	72.51 ± 0.35	71.74 ± 0.29	75.64 ± 0.21	75.45 ± 0.17
GCN*	77.29 ± 0.46 4.78 ↑	73.60 ± 0.18 1.86 ↑	82.33 ± 0.19 6.69 ↑	86.33 ± 0.17 10.88 ↑
GraphSAGE	77.68 ± 0.20	71.49 ± 0.27	78.29 ± 0.16	75.63 ± 0.38
GraphSAGE*	82.21 ± 0.32 4.53 ↑	72.95 ± 0.31 1.46 ↑	83.89 ± 0.36 5.60 ↑	85.97 ± 0.21 10.34 ↑
GAT	72.02 ± 0.44	71.95 ± 0.36	79.45 ± 0.59	72.23 ± 0.18
GAT*	85.01 ± 0.46 12.99 ↑	73.30 ± 0.16 1.35 ↑	80.99 ± 0.16 1.54 ↑	86.19 ± 0.23 13.96 ↑

Observations on Homophilous Graphs (Table 2). Classic GNNs, with only slight adjustments to hyperparameters, are highly competitive in node classification tasks on homophilous graphs, often outperforming state-of-the-art graph transformers in many cases.

While previously reported results show that most advanced GTs outperform classic GNN on homophilous graphs [12, 71], our implementation of classic GNNs can place within the top two for five datasets, with GCN* always ranking in the top three. Specifically, on CS and WikiCS, classic GNNs experience about a 3% accuracy increase, achieving top-three performances. On WikiCS, the accuracy of GAT* increases by 3.84%, moving it from seventh to first place, surpassing the leading GT, Polynormer. Similarly, on Computer and Photo, GAT* outperforms Polynormer and SGFormer, establishing itself as the top model. On Cora, CiteSeer, PubMed, and Physics, tuning yields significant performance improvements for GCN*, with accuracy increases ranging from 1.25% to 3.48%, positioning GCN* as the highest-performing model despite its initial lower accuracy compared to advanced GTs.

Observations on Heterophilous Graphs (Table 3). Our implementation has significantly enhanced the previously reported best results of classic GNNs on heterophilous graphs, surpassing specialized GNN models tailored for such graphs and even outperforming the leading graph transformer architectures. This advancement not only supports but also strengthens the findings in [54] that conventional GNNs are strong contenders for heterophilous graphs, challenging the prevailing assumption that they are primarily suited for homophilous graph structures.

The three classic GNNs consistently secure top positions on five out of six heterophilous graphs. Specifically, on well-known page-page networks like Squirrel and Chameleon, our implementation enhances the accuracy of GCN* by 4.80% and 5.83% respectively, elevating it to the first place among all models. By comparison, on larger heterophilous graphs such as Amazon-Ratings and Questions, GAT* exhibits the highest performance, highlighting the superiority of its message-passing attention mechanism over GTs’ global attention. On Roman-Empire, a 17.68% increase is observed in the performance of GCN*. Interestingly, we find that improvements primarily stem from residual connections, which are further analyzed in our ablation study (see Section 5.2).

Observations on Large-scale Graphs (Table 4). Our implementation has significantly enhanced the previously reported results of classic GNNs, with some cases showing double-digit increases in accuracy. It has achieved the best results across these large graph datasets, either homophilous or heterophilous, and has outperformed state-of-the-art graph transformers. This indicates that message passing remains highly effective for learning node representations on large-scale graphs.

Our implementation of classic GNNs demonstrate consistently superior performance, achieving top rankings across all four large-scale datasets included in our study. Notably, GCN* emerges as the leading model on ogbn-arxiv and pokec, surpassing all evaluated advanced GTs. Furthermore, on pokec, all three classic GNNs achieve over 10% performance increases by our implementation. For ogbn-proteins, an absolute improvement of 12.99% is observed in the performance of GAT*, significantly surpassing SGFormer by 5.48%. Similarly, on ogbn-products, GraphSAGE* demonstrates a performance increase, securing the best performance among all evaluated models. In summary, a basic GNN can achieve the best known results on large-scale graphs, suggesting that current GTs have not yet addressed GNN issues such as over-smoothing and long-range dependencies.

5.2 Influence of Hyperparameters on the Performance of GNNs

To examine the unique contributions of different hyperparameters in explaining the enhanced performance of classic GNNs, we conduct a series of ablation analysis by selectively removing elements such as normalization, dropout, residual connections, network depth, and jumping knowledge from GCN*, GraphSAGE*, and GAT*. The effect of these ablations is assessed across homophilous (see Table 5), heterophilous (see Table 6), and large-scale graphs (see Table 7). Our findings, which we detail below, indicate that the ablation of single components affects model accuracy in distinct ways.

Observation 1: Normalization (either BN or LN) is important for node classification on large-scale graphs but less significant on smaller-scale graphs.

Note that we do not conduct an exhaustive search regarding BN and LN, with specific choices detailed in Appendix A. We observe that the ablation of normalization does not lead to substantial deviations on small graphs. However, normalization becomes consistently crucial on large-scale graphs, where its ablation results in accuracy reductions of 3.81% and 4.69% for GraphSAGE* and GAT* respectively on ogbn-proteins. We believe this is because large graphs display a wider variety of node features, resulting in different data distributions across the graph. Normalization aids in standardizing these features during training, ensuring a more stable distribution.

Observation 2: Dropout is consistently found to be essential for node classification.

Our analysis highlights the crucial role of dropout in maintaining the performance of classic GNNs on both homophilous and heterophilous graphs, with its ablation contributing to notable accuracy declines—for instance, a 3.71% decrease for GraphSAGE* on PubMed and a 5.69% decrease on

Table 5: Ablation study on homophilous graphs (%).

	Cora	CiteSeer	PubMed	Computer	Photo	CS	Physics	WikiCS
Metric	Accuracy \uparrow	Accuracy \uparrow	Accuracy \uparrow	Accuracy \uparrow	Accuracy \uparrow	Accuracy \uparrow	Accuracy \uparrow	Accuracy \uparrow
GCN*	85.08 \pm 0.52	72.98 \pm 0.84	81.32 \pm 0.72	93.80 \pm 0.29	96.51 \pm 0.20	95.80 \pm 0.28	97.43 \pm 0.05	80.27 \pm 0.71
(-) Normalization	85.08 \pm 0.52	72.98 \pm 0.84	81.32 \pm 0.72	93.09 \pm 0.13	96.38 \pm 0.14	94.47 \pm 0.25	97.18 \pm 0.15	80.27 \pm 0.71
(-) Dropout	82.70 \pm 0.87	70.96 \pm 1.00	79.50 \pm 1.29	93.34 \pm 0.11	96.51 \pm 0.20	95.59 \pm 0.16	97.32 \pm 0.06	78.34 \pm 0.42
(-) Residual Connections	83.40 \pm 1.58	71.60 \pm 1.26	80.86 \pm 0.58	93.80 \pm 0.29	94.68 \pm 0.29	94.45 \pm 0.12	96.89 \pm 0.20	79.38 \pm 0.57
(-) Jumping Knowledge	85.08 \pm 0.52	72.98 \pm 0.84	81.32 \pm 0.72	92.97 \pm 0.08	95.93 \pm 0.32	93.73 \pm 0.53	97.00 \pm 0.10	79.13 \pm 0.91
GraphSAGE*	84.18 \pm 0.81	71.93 \pm 0.85	79.41 \pm 0.53	93.59 \pm 0.22	96.41 \pm 0.17	96.12 \pm 0.24	97.21 \pm 0.05	80.51 \pm 0.48
(-) Normalization	84.18 \pm 0.81	71.80 \pm 0.19	79.41 \pm 0.53	93.07 \pm 0.12	96.41 \pm 0.17	94.53 \pm 0.14	96.73 \pm 0.05	80.41 \pm 0.70
(-) Dropout	81.54 \pm 1.55	70.36 \pm 0.47	75.70 \pm 1.69	92.71 \pm 0.47	96.23 \pm 0.10	96.12 \pm 0.24	97.14 \pm 0.04	80.51 \pm 0.57
(-) Residual Connections	80.46 \pm 1.19	71.80 \pm 0.19	79.41 \pm 0.53	93.23 \pm 0.26	95.95 \pm 0.13	95.87 \pm 0.08	97.16 \pm 0.04	80.00 \pm 0.76
(-) Jumping Knowledge	84.18 \pm 0.81	70.00 \pm 1.26	79.41 \pm 0.53	93.16 \pm 0.18	95.82 \pm 0.10	94.67 \pm 0.26	96.91 \pm 0.04	79.89 \pm 0.79
GAT*	84.64 \pm 1.27	72.10 \pm 1.10	79.70 \pm 0.70	93.93 \pm 0.16	96.67 \pm 0.13	96.08 \pm 0.10	97.30 \pm 0.06	80.75 \pm 0.74
(-) Normalization	84.64 \pm 1.27	72.10 \pm 1.10	79.70 \pm 0.70	93.86 \pm 0.10	96.21 \pm 0.17	94.50 \pm 0.33	96.99 \pm 0.15	80.75 \pm 0.74
(-) Dropout	83.18 \pm 1.16	70.82 \pm 0.76	79.04 \pm 0.44	93.35 \pm 0.33	96.67 \pm 0.13	95.85 \pm 0.04	97.30 \pm 0.06	80.19 \pm 0.16
(-) Residual Connections	83.34 \pm 0.24	71.88 \pm 0.40	79.70 \pm 0.70	93.29 \pm 0.31	95.29 \pm 0.13	94.47 \pm 0.25	96.51 \pm 0.05	79.30 \pm 0.92
(-) Jumping Knowledge	82.78 \pm 0.96	70.36 \pm 0.44	79.70 \pm 0.70	93.44 \pm 0.22	96.43 \pm 0.20	94.41 \pm 0.28	97.03 \pm 0.04	79.56 \pm 1.31

Table 6: Ablation study on heterophilous graphs (%).

	Squirrel	Chameleon	Amazon-Ratings	Roman-Empire	Minesweeper	Questions
Metric	Accuracy \uparrow	Accuracy \uparrow	Accuracy \uparrow	Accuracy \uparrow	ROC-AUC \uparrow	ROC-AUC \uparrow
GCN*	44.50 \pm 1.92	46.11 \pm 3.16	53.57 \pm 0.32	91.35 \pm 0.37	97.77 \pm 0.38	77.40 \pm 1.07
(-) Normalization	43.92 \pm 1.59	46.11 \pm 3.16	53.57 \pm 0.32	91.35 \pm 0.37	97.77 \pm 0.38	77.40 \pm 1.07
(-) Dropout	41.96 \pm 1.89	46.11 \pm 3.16	50.99 \pm 0.21	86.88 \pm 0.34	94.33 \pm 0.21	76.92 \pm 1.55
(-) Residual Connections	44.50 \pm 1.92	43.22 \pm 3.91	50.31 \pm 0.25	75.63 \pm 0.48	89.16 \pm 0.24	74.49 \pm 0.39
(-) Jumping Knowledge	43.10 \pm 1.47	43.81 \pm 3.96	51.63 \pm 0.27	90.73 \pm 0.25	95.29 \pm 0.62	77.30 \pm 0.57
GraphSAGE*	39.93 \pm 1.58	43.44 \pm 3.19	54.72 \pm 0.38	92.19 \pm 0.58	96.95 \pm 0.41	77.96 \pm 0.72
(-) Normalization	39.93 \pm 1.58	43.44 \pm 3.19	54.50 \pm 0.38	92.19 \pm 0.58	96.95 \pm 0.41	76.07 \pm 1.56
(-) Dropout	39.93 \pm 1.58	40.98 \pm 4.65	52.58 \pm 0.17	86.50 \pm 0.13	93.92 \pm 0.73	77.96 \pm 0.72
(-) Residual Connections	39.37 \pm 2.30	41.24 \pm 3.85	53.94 \pm 0.40	88.65 \pm 0.96	94.41 \pm 0.43	76.70 \pm 0.87
(-) Jumping Knowledge	38.70 \pm 1.95	43.44 \pm 3.19	54.27 \pm 0.69	90.12 \pm 0.54	93.80 \pm 0.30	76.80 \pm 0.72
GAT*	38.72 \pm 1.46	43.44 \pm 3.00	54.99 \pm 0.71	91.60 \pm 0.21	97.76 \pm 0.37	79.04 \pm 1.27
(-) Normalization	38.72 \pm 1.46	42.24 \pm 3.26	54.99 \pm 0.71	90.96 \pm 0.20	97.76 \pm 0.37	79.02 \pm 1.13
(-) Dropout	38.72 \pm 1.46	41.08 \pm 2.96	53.84 \pm 0.87	87.06 \pm 0.21	94.10 \pm 0.09	78.51 \pm 0.36
(-) Residual Connections	38.72 \pm 1.46	41.74 \pm 2.08	51.24 \pm 0.28	79.11 \pm 0.88	90.83 \pm 0.45	77.07 \pm 0.84
(-) Jumping Knowledge	38.72 \pm 1.46	41.12 \pm 3.94	54.38 \pm 0.29	91.60 \pm 0.21	93.92 \pm 0.73	79.04 \pm 1.27

Roman-Empire. This trend persists in large-scale datasets, where the ablation of dropout leads to a 2.44% and 2.53% performance decline for GCN* and GAT* respectively on ogbn-proteins.

Observation 3: Residual connections can significantly boost performance on specific datasets, exhibiting a more pronounced effect on heterophilous graphs than on homophilous graphs.

While the ablation of residual connections on homophilous graphs does not consistently lead to a significant performance decrease, with observed differences around 2% on Cora, Photo, and CS, the impact is more substantial on large-scale graphs such as ogbn-proteins and pokec. The effect is even more dramatic on heterophilous graphs, with the classic GNNs exhibiting the most significant accuracy reduction on Roman-Empire, for instance, a 15.72% for GCN* and 12.49% for GAT*. Similarly, on Minesweeper, significant performance drops were observed, emphasizing the critical importance of residual connections, particularly on heterophilous graphs. The complex structures of these graphs often necessitate deeper layers to effectively capture the diverse relationships between nodes. In such contexts, residual connections are essential for model training.

Observation 4: Deeper networks generally lead to greater performance gains on heterophilous graphs compared to homophilous graphs.

As demonstrated in Figure 1, the performance trends for GCN* and GraphSAGE* are consistent across different graph types. On homophilous graphs and ogbn-arxiv, both models achieve optimal performance with a range of 4 to 8 layers. In contrast, on heterophilous graphs, their performance improves with an increasing number of layers, indicating that deeper networks are more beneficial for these graphs. We discuss scenarios with more than 10 layers in Appendix B.

Observation 5: Jumping knowledge mode has minimal influence on large-scale graphs.

Table 7: Ablation study on large-scale graphs (%).

	ogbn-proteins	ogbn-arxiv	ogbn-products	pokec
Metric	ROC-AUC↑	Accuracy↑	Accuracy↑	Accuracy↑
GCN*	77.29 ± 0.46	73.60 ± 0.18	82.33 ± 0.19	86.33 ± 0.17
(-) Normalization	74.48 ± 1.13	71.97 ± 0.18	80.01 ± 0.48	85.21 ± 0.23
(-) Dropout	74.85 ± 0.87	72.59 ± 0.23	79.30 ± 0.37	84.47 ± 0.38
(-) Residual Connections	73.19 ± 1.46	73.01 ± 0.09	82.33 ± 0.19	79.59 ± 0.97
(-) Jumping Knowledge	77.29 ± 0.46	72.98 ± 0.24	82.33 ± 0.19	86.33 ± 0.17
GraphSAGE*	82.21 ± 0.32	72.95 ± 0.31	83.89 ± 0.36	85.97 ± 0.21
(-) Normalization	77.42 ± 0.98	71.52 ± 0.17	82.12 ± 0.31	84.95 ± 0.33
(-) Dropout	80.52 ± 0.49	71.51 ± 0.04	80.36 ± 0.43	83.06 ± 0.28
(-) Residual Connections	81.75 ± 0.53	72.84 ± 0.09	83.89 ± 0.36	85.81 ± 0.45
(-) Jumping Knowledge	82.21 ± 0.32	72.76 ± 0.17	83.89 ± 0.36	85.97 ± 0.21
GAT*	85.01 ± 0.46	73.30 ± 0.16	80.99 ± 0.16	86.19 ± 0.23
(-) Normalization	80.32 ± 0.83	71.68 ± 0.36	78.62 ± 0.33	84.63 ± 0.64
(-) Dropout	82.48 ± 0.34	71.83 ± 0.42	77.68 ± 0.21	85.12 ± 0.49
(-) Residual Connections	82.43 ± 0.75	72.76 ± 0.45	80.99 ± 0.16	81.37 ± 0.87
(-) Jumping Knowledge	85.01 ± 0.46	72.94 ± 0.30	80.99 ± 0.16	86.19 ± 0.23

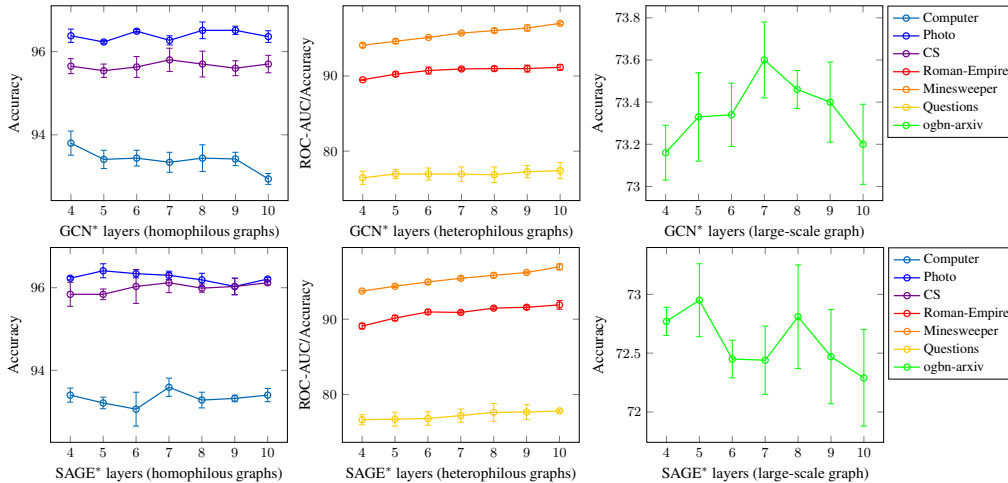


Figure 1: Ablation studies of the number of layers showing, from left to right, results for homophilous graphs, heterophilous graphs, and large-scale graphs, respectively.

The ablation of this component typically results in marginal accuracy decreases of less than 0.5% for classic GNNs across large-scale graphs, suggesting the lesser impact of jumping knowledge than other components. By comparison, on smaller-scale homophilous graphs, such as CiteSeer and CS, the ablation of jumping knowledge can lead to decreases of around 1.5 to 2% in the model performance. On some heterophilous graphs, the effect is also significant, with the accuracy of GAT* decreasing by 2.32% on Chameleon, GraphSAGE* by 3.15% and GAT* by 3.84% on Minesweeper.

6 Conclusion

Our study provides a thorough reevaluation of the efficacy of foundational GNN models in node classification tasks. Through extensive empirical analysis, we demonstrate that these classic GNN models can reach or surpass the performance of GTs on various graph datasets, challenging the perceived superiority of GTs in node classification tasks. Furthermore, our comprehensive ablation studies provide insights into how various GNN configurations impact performance. We hope our findings promote more rigorous empirical evaluations in graph machine learning research.

References

- [1] Uri Alon and Eran Yahav. On the bottleneck of graph neural networks and its practical implications. *arXiv preprint arXiv:2006.05205*, 2020.
- [2] Jimmy Lei Ba, Jamie Ryan Kiros, and Geoffrey E Hinton. Layer normalization. *arXiv preprint arXiv:1607.06450*, 2016.
- [3] Deyu Bo, Chuan Shi, Lele Wang, and Renjie Liao. Specformer: Spectral graph neural networks meet transformers. *arXiv preprint arXiv:2303.01028*, 2023.
- [4] Xavier Bresson and Thomas Laurent. Residual gated graph convnets. *arXiv preprint arXiv:1711.07553*, 2017.
- [5] Tianle Cai, Shengjie Luo, Keyulu Xu, Di He, Tie-yan Liu, and Liwei Wang. Graphnorm: A principled approach to accelerating graph neural network training. In *International Conference on Machine Learning*, pages 1204–1215. PMLR, 2021.
- [6] Dexiong Chen, Leslie O’Bray, and Karsten Borgwardt. Structure-aware transformer for graph representation learning. In *International Conference on Machine Learning*, pages 3469–3489. PMLR, 2022.
- [7] Jinsong Chen, Kaiyuan Gao, Gaichao Li, and Kun He. Nagphormer: A tokenized graph transformer for node classification in large graphs. In *The Eleventh International Conference on Learning Representations*, 2022.
- [8] Ming Chen, Zhewei Wei, Zengfeng Huang, Bolin Ding, and Yaliang Li. Simple and deep graph convolutional networks. In *International conference on machine learning*, pages 1725–1735. PMLR, 2020.
- [9] Eli Chien, Jianhao Peng, Pan Li, and Olgica Milenkovic. Adaptive universal generalized pagerank graph neural network. In *International Conference on Learning Representations*, 2020.
- [10] Gabriele Corso, Luca Cavalleri, Dominique Beaini, Pietro Liò, and Petar Veličković. Principal neighbourhood aggregation for graph nets. *Advances in Neural Information Processing Systems*, 33:13260–13271, 2020.
- [11] Hanjun Dai, Zornitsa Kozareva, Bo Dai, Alex Smola, and Le Song. Learning steady-states of iterative algorithms over graphs. In *International conference on machine learning*, pages 1106–1114. PMLR, 2018.
- [12] Chenhui Deng, Zichao Yue, and Zhiru Zhang. Polynormer: Polynomial-expressive graph transformer in linear time. *arXiv preprint arXiv:2403.01232*, 2024.
- [13] Vijay Prakash Dwivedi and Xavier Bresson. A generalization of transformer networks to graphs. *arXiv preprint arXiv:2012.09699*, 2020.
- [14] Vijay Prakash Dwivedi, Chaitanya K Joshi, Anh Tuan Luu, Thomas Laurent, Yoshua Bengio, and Xavier Bresson. Benchmarking graph neural networks. *Journal of Machine Learning Research*, 24(43):1–48, 2023.
- [15] Vijay Prakash Dwivedi, Yozen Liu, Anh Tuan Luu, Xavier Bresson, Neil Shah, and Tong Zhao. Graph transformers for large graphs. *arXiv preprint arXiv:2312.11109*, 2023.
- [16] Matthias Fey and Jan Eric Lenssen. Fast graph representation learning with pytorch geometric. *arXiv preprint arXiv:1903.02428*, 2019.
- [17] Dongqi Fu, Zhigang Hua, Yan Xie, Jin Fang, Si Zhang, Kaan Sancak, Hao Wu, Andrey Malevich, Jingrui He, and Bo Long. VCR-graphormer: A mini-batch graph transformer via virtual connections. In *The Twelfth International Conference on Learning Representations*, 2024.
- [18] Johannes Gasteiger, Aleksandar Bojchevski, and Stephan Günnemann. Predict then propagate: Graph neural networks meet personalized pagerank. *arXiv preprint arXiv:1810.05997*, 2018.

- [19] Justin Gilmer, Samuel S Schoenholz, Patrick F Riley, Oriol Vinyals, and George E Dahl. Neural message passing for quantum chemistry. In *International conference on machine learning*, pages 1263–1272. PMLR, 2017.
- [20] Will Hamilton, Zhitao Ying, and Jure Leskovec. Inductive representation learning on large graphs. *Advances in neural information processing systems*, 30, 2017.
- [21] Kaiming He, Xiangyu Zhang, Shaoqing Ren, and Jian Sun. Deep residual learning for image recognition. In *Proceedings of the IEEE conference on computer vision and pattern recognition*, pages 770–778, 2016.
- [22] Geoffrey E Hinton, Nitish Srivastava, Alex Krizhevsky, Ilya Sutskever, and Ruslan R Salakhutdinov. Improving neural networks by preventing co-adaptation of feature detectors. *arXiv preprint arXiv:1207.0580*, 2012.
- [23] Van Thuy Hoang, O Lee, et al. A survey on structure-preserving graph transformers. *arXiv preprint arXiv:2401.16176*, 2024.
- [24] Weihua Hu, Matthias Fey, Marinka Zitnik, Yuxiao Dong, Hongyu Ren, Bowen Liu, Michele Catasta, and Jure Leskovec. Open graph benchmark: Datasets for machine learning on graphs. *Advances in neural information processing systems*, 33:22118–22133, 2020.
- [25] Gao Huang, Zhuang Liu, Laurens Van Der Maaten, and Kilian Q Weinberger. Densely connected convolutional networks. In *Proceedings of the IEEE conference on computer vision and pattern recognition*, pages 4700–4708, 2017.
- [26] Sergey Ioffe and Christian Szegedy. Batch normalization: Accelerating deep network training by reducing internal covariate shift. In *International conference on machine learning*, pages 448–456. pmlr, 2015.
- [27] Diederik P Kingma and Jimmy Ba. Adam: A method for stochastic optimization. *arXiv preprint arXiv:1412.6980*, 2014.
- [28] Thomas N. Kipf and Max Welling. Semi-supervised classification with graph convolutional networks. In *International Conference on Learning Representations*, 2017.
- [29] Kezhi Kong, Jiuhai Chen, John Kirchenbauer, Renkun Ni, C. Bayan Bruss, and Tom Goldstein. GOAT: A global transformer on large-scale graphs. In Andreas Krause, Emma Brunskill, Kyunghyun Cho, Barbara Engelhardt, Sivan Sabato, and Jonathan Scarlett, editors, *Proceedings of the 40th International Conference on Machine Learning*, volume 202 of *Proceedings of Machine Learning Research*, pages 17375–17390. PMLR, 23–29 Jul 2023.
- [30] Devin Kreuzer, Dominique Beaini, Will Hamilton, Vincent Létourneau, and Prudencio Tossou. Rethinking graph transformers with spectral attention. *Advances in Neural Information Processing Systems*, 34:21618–21629, 2021.
- [31] Weirui Kuang, WANG Zhen, Yaliang Li, Zhewei Wei, and Bolin Ding. Coarformer: Transformer for large graph via graph coarsening. 2021.
- [32] Jure Leskovec and Andrej Krevl. Snap datasets: Stanford large network dataset collection. 2014. 2016.
- [33] Guohao Li, Matthias Muller, Ali Thabet, and Bernard Ghanem. Deepgcns: Can gcns go as deep as cnns? In *Proceedings of the IEEE/CVF international conference on computer vision*, pages 9267–9276, 2019.
- [34] Guohao Li, Chenxin Xiong, Ali Thabet, and Bernard Ghanem. Deepergcn: All you need to train deeper gcns. *arXiv preprint arXiv:2006.07739*, 2020.
- [35] Qimai Li, Zhichao Han, and Xiao-Ming Wu. Deeper insights into graph convolutional networks for semi-supervised learning. In *Thirty-Second AAAI conference on artificial intelligence*, 2018.

- [36] Xiang Li, Renyu Zhu, Yao Cheng, Caihua Shan, Siqiang Luo, Dongsheng Li, and Weining Qian. Finding global homophily in graph neural networks when meeting heterophily. In *International Conference on Machine Learning*, pages 13242–13256. PMLR, 2022.
- [37] Derek Lim, Felix Hohne, Xiuyu Li, Sijia Linda Huang, Vaishnavi Gupta, Omkar Bhalerao, and Ser Nam Lim. Large scale learning on non-homophilous graphs: New benchmarks and strong simple methods. *Advances in Neural Information Processing Systems*, 34:20887–20902, 2021.
- [38] Chuang Liu, Yibing Zhan, Xueqi Ma, Liang Ding, Dapeng Tao, Jia Wu, and Wenbin Hu. Gapformer: Graph transformer with graph pooling for node classification. In *Proceedings of the Thirty-Second International Joint Conference on Artificial Intelligence, IJCAI*, pages 2196–2205, 2023.
- [39] Sitao Luan, Chenqing Hua, Qincheng Lu, Jiaqi Zhu, Mingde Zhao, Shuyuan Zhang, Xiao-Wen Chang, and Doina Precup. Revisiting heterophily for graph neural networks. *Advances in neural information processing systems*, 35:1362–1375, 2022.
- [40] Yuankai Luo, Hongkang Li, Lei Shi, and Xiao-Ming Wu. Enhancing graph transformers with hierarchical distance structural encoding. *arXiv preprint arXiv:2308.11129*, 2024.
- [41] Yuankai Luo, Qijiong Liu, Lei Shi, and Xiao-Ming Wu. Structure-aware semantic node identifiers for learning on graphs. *arXiv preprint arXiv:2405.16435*, 2024.
- [42] Yuankai Luo, Veronika Thost, and Lei Shi. Transformers over directed acyclic graphs. *Advances in Neural Information Processing Systems*, 36, 2024.
- [43] Yao Ma, Xiaorui Liu, Neil Shah, and Jiliang Tang. Is homophily a necessity for graph neural networks? *arXiv preprint arXiv:2106.06134*, 2021.
- [44] Seiji Maekawa, Koki Noda, Yuya Sasaki, et al. Beyond real-world benchmark datasets: An empirical study of node classification with gnns. *Advances in Neural Information Processing Systems*, 35:5562–5574, 2022.
- [45] Sunil Kumar Maurya, Xin Liu, and Tsuyoshi Murata. Improving graph neural networks with simple architecture design. *arXiv preprint arXiv:2105.07634*, 2021.
- [46] Sunil Kumar Maurya, Xin Liu, and Tsuyoshi Murata. Simplifying approach to node classification in graph neural networks. *Journal of Computational Science*, 62:101695, 2022.
- [47] Péter Mernyei and Cătălina Cangea. Wiki-cs: A wikipedia-based benchmark for graph neural networks. *arXiv preprint arXiv:2007.02901*, 2020.
- [48] Erxue Min, Runfa Chen, Yatao Bian, Tingyang Xu, Kangfei Zhao, Wenbing Huang, Peilin Zhao, Junzhou Huang, Sophia Ananiadou, and Yu Rong. Transformer for graphs: An overview from architecture perspective. *arXiv preprint arXiv:2202.08455*, 2022.
- [49] Christopher Morris, Martin Ritzert, Matthias Fey, William L Hamilton, Jan Eric Lenssen, Gaurav Rattan, and Martin Grohe. Weisfeiler and leman go neural: Higher-order graph neural networks. In *Proceedings of the AAAI conference on artificial intelligence*, volume 33, pages 4602–4609, 2019.
- [50] Luis Müller, Mikhail Galkin, Christopher Morris, and Ladislav Rampásek. Attending to graph transformers. *arXiv preprint arXiv:2302.04181*, 2023.
- [51] Mathias Niepert, Mohamed Ahmed, and Konstantin Kutzkov. Learning convolutional neural networks for graphs. In *International conference on machine learning*, pages 2014–2023. PMLR, 2016.
- [52] Giannis Nikolentzos and Michalis Vazirgiannis. Random walk graph neural networks. *Advances in Neural Information Processing Systems*, 33:16211–16222, 2020.
- [53] Hongbin Pei, Bingzhe Wei, Kevin Chen-Chuan Chang, Yu Lei, and Bo Yang. Geom-gcn: Geometric graph convolutional networks. *arXiv preprint arXiv:2002.05287*, 2020.

- [54] Oleg Platonov, Denis Kuznedelev, Michael Diskin, Artem Babenko, and Liudmila Prokhorenkova. A critical look at the evaluation of gnns under heterophily: Are we really making progress? *arXiv preprint arXiv:2302.11640*, 2023.
- [55] Ladislav Rampásek, Mikhail Galkin, Vijay Prakash Dwivedi, Anh Tuan Luu, Guy Wolf, and Dominique Beaini. Recipe for a general, powerful, scalable graph transformer. *arXiv preprint arXiv:2205.12454*, 2022.
- [56] Emanuele Rossi, Fabrizio Frasca, Ben Chamberlain, Davide Eynard, Michael Bronstein, and Federico Monti. Sign: Scalable inception graph neural networks. *arXiv preprint arXiv:2004.11198*, 7:15, 2020.
- [57] Benedek Rozemberczki, Carl Allen, and Rik Sarkar. Multi-scale attributed node embedding. *Journal of Complex Networks*, 9(2):cnab014, 2021.
- [58] Prithviraj Sen, Galileo Namata, Mustafa Bilgic, Lise Getoor, Brian Galligher, and Tina Eliassi-Rad. Collective classification in network data. *AI magazine*, 29(3):93–93, 2008.
- [59] Oleksandr Shchur, Maximilian Mumme, Aleksandar Bojchevski, and Stephan Günnemann. Pitfalls of graph neural network evaluation. *arXiv preprint arXiv:1811.05868*, 2018.
- [60] Hamed Shirzad, Ameya Velingker, Balaji Venkatachalam, Danica J Sutherland, and Ali Kemal Sinop. Exphormer: Sparse transformers for graphs. *arXiv preprint arXiv:2303.06147*, 2023.
- [61] Juan Shu, Bowei Xi, Yu Li, Fan Wu, Charles Kamhoua, and Jianzhu Ma. Understanding dropout for graph neural networks. In *Companion Proceedings of the Web Conference 2022*, pages 1128–1138, 2022.
- [62] Yunchong Song, Chenghu Zhou, Xinbing Wang, and Zhouhan Lin. Ordered GNN: Ordering message passing to deal with heterophily and over-smoothing. In *The Eleventh International Conference on Learning Representations*, 2023.
- [63] Nitish Srivastava, Geoffrey Hinton, Alex Krizhevsky, Ilya Sutskever, and Ruslan Salakhutdinov. Dropout: a simple way to prevent neural networks from overfitting. *The journal of machine learning research*, 15(1):1929–1958, 2014.
- [64] Ashish Vaswani, Noam Shazeer, Niki Parmar, Jakob Uszkoreit, Llion Jones, Aidan N Gomez, Lukasz Kaiser, and Illia Polosukhin. Attention is all you need. *Advances in neural information processing systems*, 30, 2017.
- [65] Petar Veličković, Guillem Cucurull, Arantxa Casanova, Adriana Romero, Pietro Liò, and Yoshua Bengio. Graph attention networks. In *International Conference on Learning Representations*, 2018.
- [66] Clement Vignac, Andreas Loukas, and Pascal Frossard. Building powerful and equivariant graph neural networks with structural message-passing. *Advances in neural information processing systems*, 33:14143–14155, 2020.
- [67] Minjie Wang, Da Zheng, Zihao Ye, Quan Gan, Mufei Li, Xiang Song, Jinjing Zhou, Chao Ma, Lingfan Yu, Yu Gai, et al. Deep graph library: A graph-centric, highly-performant package for graph neural networks. *arXiv preprint arXiv:1909.01315*, 2019.
- [68] Yangkun Wang, Jiarui Jin, Weinan Zhang, Yong Yu, Zheng Zhang, and David Wipf. Bag of tricks for node classification with graph neural networks. *arXiv preprint arXiv:2103.13355*, 2021.
- [69] Qitian Wu, Chenxiao Yang, Wentao Zhao, Yixuan He, David Wipf, and Junchi Yan. DIF-Former: Scalable (graph) transformers induced by energy constrained diffusion. In *The Eleventh International Conference on Learning Representations*, 2023.
- [70] Qitian Wu, Wentao Zhao, Zenan Li, David P Wipf, and Junchi Yan. Nodeformer: A scalable graph structure learning transformer for node classification. *Advances in Neural Information Processing Systems*, 35:27387–27401, 2022.

- [71] Qitian Wu, Wentao Zhao, Chenxiao Yang, Hengrui Zhang, Fan Nie, Haitian Jiang, Yatao Bian, and Junchi Yan. Simplifying and empowering transformers for large-graph representations. In *Thirty-seventh Conference on Neural Information Processing Systems, 2023*.
- [72] Keyulu Xu, Weihua Hu, Jure Leskovec, and Stefanie Jegelka. How powerful are graph neural networks? *arXiv preprint arXiv:1810.00826*, 2018.
- [73] Keyulu Xu, Chengtao Li, Yonglong Tian, Tomohiro Sonobe, Ken-ichi Kawarabayashi, and Stefanie Jegelka. Representation learning on graphs with jumping knowledge networks. In *International conference on machine learning*, pages 5453–5462. PMLR, 2018.
- [74] Chengxuan Ying, Tianle Cai, Shengjie Luo, Shuxin Zheng, Guolin Ke, Di He, Yanming Shen, and Tie-Yan Liu. Do transformers really perform badly for graph representation? *Advances in Neural Information Processing Systems*, 34:28877–28888, 2021.
- [75] Jason Yosinski, Jeff Clune, Yoshua Bengio, and Hod Lipson. How transferable are features in deep neural networks? *Advances in neural information processing systems*, 27, 2014.
- [76] Jiaxuan You, Rex Ying, and Jure Leskovec. Position-aware graph neural networks. In *International conference on machine learning*, pages 7134–7143. PMLR, 2019.
- [77] Seongjun Yun, Seoyoon Kim, Junhyun Lee, Jaewoo Kang, and Hyunwoo J Kim. Neo-gnns: Neighborhood overlap-aware graph neural networks for link prediction. *Advances in Neural Information Processing Systems*, 34:13683–13694, 2021.
- [78] Bohang Zhang, Shengjie Luo, Liwei Wang, and Di He. Rethinking the expressive power of GNNs via graph biconnectivity. In *The Eleventh International Conference on Learning Representations, 2023*.
- [79] Zaixi Zhang, Qi Liu, Qingyong Hu, and Chee-Kong Lee. Hierarchical graph transformer with adaptive node sampling. *Advances in Neural Information Processing Systems*, 35:21171–21183, 2022.
- [80] Jiong Zhu, Ryan A Rossi, Anup Rao, Tung Mai, Nedim Lipka, Nesreen K Ahmed, and Danai Koutra. Graph neural networks with heterophily. In *Proceedings of the AAAI conference on artificial intelligence*, volume 35, pages 11168–11176, 2021.
- [81] Jiong Zhu, Yujun Yan, Lingxiao Zhao, Mark Heimann, Leman Akoglu, and Danai Koutra. Beyond homophily in graph neural networks: Current limitations and effective designs. *Advances in neural information processing systems*, 33:7793–7804, 2020.
- [82] Wenhao Zhu, Tianyu Wen, Guojie Song, Xiaojun Ma, and Liang Wang. Hierarchical transformer for scalable graph learning. *arXiv preprint arXiv:2305.02866*, 2023.

A Datasets and Experimental Details

A.1 Computing Environment

Our implementation is based on PyG [16] and DGL [67]. The experiments are conducted on a single workstation with 8 RTX 3090 GPUs.

A.2 Hyperparameters and Reproducibility

For the hyperparameter selections of classic GNNs, in addition to what we have covered, we list other settings in Tables 8, 9, 10. Notably, for heterophilous graphs, we expand the search range for the number of layers to include three additional settings: {11, 12, 15, 20} (See Sec. B.2 for further analysis). This adjustment is based on our empirical evidence suggesting that deep networks tend to yield performance improvements on heterophilous graphs. The ReLU function serves as the non-linear activation. Further details regarding hyperparameters can be found in our code <https://github.com/LUOyk1999/tunedGNN>.

Due to the large size of the graphs in ogbn-proteins, ogbn-products, and pokec, which prevents full-batch training on GPU memory, we adopt different training strategies. For ogbn-proteins, we utilize the optimized neighbor sampling method [20]. For pokec and ogbn-products, we apply the random partitioning method previously used by GTs [12, 71, 70] to enable mini-batch training. For other datasets, we employ full-batch training. In all experiments, we use the validation set to select the best hyperparameters. GNN* denotes our implementation of the GNN model.

Our code is available under the MIT License.

Table 8: Dataset-specific hyperparameter settings of GCN*.

Dataset	JK	ResNet	Normalization	Dropout rate	GNNs layer L	Hidden dim	LR	epoch
Cora	False	True	False	0.5	3	256	0.005	500
Citeseer	False	True	False	0.5	3	256	0.005	500
Pubmed	False	True	False	0.5	2	64	0.01	500
Computer	True	False	LN	0.7	4	512	0.001	1000
Photo	True	True	LN	0.0	9	512	0.001	1000
CS	True	True	LN	0.3	7	512	0.001	1500
Physics	True	True	LN	0.5	9	512	0.001	1500
WikiCS	True	True	False	0.5	10	512	0.001	1000
Squirrel	True	False	BN	0.5	8	64	0.01	500
Chameleon	True	True	BN	0.5	5	256	0.01	200
Amazon-Ratings	True	True	False	0.3	10	512	0.001	2500
Roman-Empire	True	True	False	0.3	11	512	0.001	2500
Minesweeper	True	True	False	0.3	15	512	0.001	2000
Questions	True	True	False	0.2	11	512	0.001	1500
ogbn-proteins	False	True	BN	0.3	3	512	0.01	100
ogbn-arxiv	True	True	BN	0.5	6	256	0.0005	2000
ogbn-products	False	False	LN	0.5	5	256	0.003	300
pokec	False	True	BN	0.2	7	256	0.0005	2000

B Additional Benchmark Results

B.1 GAT* with Edge Features on ogbn-proteins

While DeepGCN [33] introduced training models up to 56 layers deep and DeeperGCN [34] further extended this to 112 layers, our experiments suggest that such depth is not necessary. Specifically, while the DeeperGCN achieved an accuracy of 85.50% on ogbn-proteins, it utilized edge features as input, a configuration not commonly employed in the standard baselines of the OGB dataset [24]. As our experiments do not incorporate edge features on ogbn-proteins, we exclude DeeperGCN from our main text to maintain a fair comparison.

Now we incorporate edge features into the GAT*, same as the approach in [68], with the results shown in Table 11. A 6-layer GAT achieve an accuracy of 87.47%, significantly surpassing the 85.50% by DeeperGCN. This demonstrates that GNNs do not need to be as deep as proposed by DeeperGCN; a range of 2 to 10 layers is typically sufficient.

Table 9: Dataset-specific hyperparameter settings of GraphSAGE*.

Dataset	JK	ResNet	Normalization	Dropout rate	GNNs layer L	Hidden dim	LR	epoch
Cora	False	True	False	0.5	6	256	0.005	500
Citeseer	True	False	False	0.5	5	256	0.001	500
Pubmed	False	False	False	0.5	3	256	0.001	500
Computer	True	True	LN	0.7	7	512	0.001	1000
Photo	True	True	False	0.7	5	512	0.001	1000
CS	True	True	LN	0.0	7	512	0.001	1500
Physics	True	True	LN	0.5	4	512	0.001	1500
WikiCS	True	True	LN	0.5	5	512	0.001	1000
Squirrel	True	True	False	0.0	2	64	0.005	500
Chameleon	False	True	False	0.5	4	256	0.001	200
Amazon-Ratings	True	True	LN	0.3	5	512	0.001	2500
Roman-Empire	True	True	False	0.3	11	512	0.001	2500
Minesweeper	True	True	False	0.3	11	512	0.001	2000
Questions	True	True	LN	0.0	11	512	0.001	1500
ogbn-proteins	False	True	BN	0.3	6	512	0.01	1000
ogbn-arxiv	True	True	BN	0.5	7	256	0.0005	2000
ogbn-products	False	False	LN	0.5	5	256	0.003	1000
pokec	False	True	BN	0.2	7	256	0.0005	2000

Table 10: Dataset-specific hyperparameter settings of GAT*.

Dataset	JK	ResNet	Normalization	Dropout rate	GNNs layer L	Hidden dim	LR	epoch
Cora	True	True	False	0.5	6	256	0.001	500
Citeseer	True	False	False	0.5	4	256	0.001	500
Pubmed	False	False	False	0.5	2	256	0.001	500
Computer	True	True	LN	0.7	6	512	0.001	1000
Photo	True	True	LN	0.0	5	512	0.001	1000
CS	True	True	LN	0.3	5	512	0.001	1500
Physics	True	True	LN	0.0	5	512	0.001	1500
WikiCS	True	True	False	0.5	7	512	0.001	1000
Squirrel	False	False	False	0.0	3	256	0.001	500
Chameleon	True	True	BN	0.5	4	256	0.005	200
Amazon-Ratings	True	True	False	0.3	7	512	0.001	2500
Roman-Empire	False	True	LN	0.3	6	512	0.001	2500
Minesweeper	True	True	False	0.3	15	512	0.001	2000
Questions	False	True	LN	0.2	4	512	0.001	1500
ogbn-proteins	False	True	BN	0.3	7	512	0.01	1000
ogbn-arxiv	True	True	BN	0.5	6	256	0.0005	2000
ogbn-products	False	False	LN	0.5	5	256	0.003	1000
pokec	False	True	BN	0.2	7	256	0.0005	2000

B.2 Deeper Networks on Heterophilous Graphs

On heterophilous graphs, the performance of classic GNNs improves with an increasing number of layers limited to 10, as evidenced by Figure 1 in the main text. We explore scenarios with more than 10 layers in this subsection. Specifically, we consider GCN* and GAT* with layer configurations of 11, 12, 15, and 20 for the Amazon-Ratings, Roman-Empire, and Minesweeper datasets. The results are shown in Table 12. The variation in the optimal number of layers (L) could stem from the distinct structures inherent in different graphs. Heterophilous graphs may have more complex structures, thus necessitating a higher L . However, the slight improvements observed with larger L values suggest that very deep networks may not yield significantly better results. Overall, the best results for classic GNNs are achieved when L is limited to 15.

C Limitations & Broader Impacts

Broader Impacts. This paper presents work whose goal is to advance the field of Machine Learning. There are many potential societal consequences of our work, none which we feel must be specifically highlighted here.

Limitations. In this study, we focus solely on the node classification task, without delving into graph classification and link prediction tasks. It would be beneficial to extend our benchmarking efforts to include classic GNNs in graph-level and edge-level tasks. Additionally, we did not conduct an exhaustive hyperparameter search due to the large set of hyperparameters and datasets. Therefore,

Table 11: Node classification results on ogbn-proteins (%).

	ogbn-proteins
Metric	ROC-AUC↑
DeeperGCN	85.80 ± 0.17
GAT* (with edge features)	87.82 ± 0.16

Table 12: Ablation study of the number of layers L on heterophilous graphs (%).

	Amazon-Ratings	Roman-Empire	Minesweeper
Metric	Accuracy↑	Accuracy↑	ROC-AUC↑
GCN* ($L = 11$)	53.52 ± 0.19	91.35 ± 0.37	97.01 ± 0.18
GCN* ($L = 12$)	53.66 ± 0.11	90.75 ± 0.37	97.16 ± 0.28
GCN* ($L = 15$)	53.65 ± 1.02	91.10 ± 0.41	97.77 ± 0.38
GCN* ($L = 20$)	53.50 ± 0.58	91.10 ± 0.76	97.76 ± 0.30
GAT* ($L = 11$)	54.61 ± 0.21	91.07 ± 0.40	97.11 ± 0.09
GAT* ($L = 12$)	54.55 ± 0.18	90.79 ± 0.44	97.59 ± 0.15
GAT* ($L = 15$)	55.01 ± 0.45	90.98 ± 0.41	97.76 ± 0.37
GAT* ($L = 20$)	55.01 ± 0.17	91.30 ± 0.38	97.56 ± 0.47

future research could potentially uncover more favourable results by undertaking a more comprehensive exploration of the hyperparameter space.